JVI Journals.ASM.org

Murine Leukemia Virus Uses NXF1 for Nuclear Export of Spliced and Unspliced Viral Transcripts

Toshie Sakuma,[a] Jaime I. Davila,[b] Jessica A. Malcolm,[a] Jean-Pierre A. Kocher,[b] Jason M. Tonne,[a] Yasuhiro Ikeda[a]

Department of Molecular Medicine, Mayo Clinic, Rochester, Minnesota, USA[a]; Department of Health Sciences Research, Mayo Clinic, Rochester, Minnesota, USA[b]

ABSTRACT

Intron-containing mRNAs are subject to restricted nuclear export in higher eukaryotes. Retroviral replication requires the nucleocytoplasmic transport of both spliced and unspliced RNA transcripts, and RNA export mechanisms of gammaretroviruses are poorly characterized. Here, we report the involvement of the nuclear export receptor NXF1/TAP in the nuclear export of gammaretroviral RNA transcripts. We identified a conserved *cis*-acting element in the *pol* gene of gammaretroviruses, including murine leukemia virus (MLV) and xenotropic murine leukemia virus (XMRV), named the CAE (cytoplasmic accumulation element). The CAE enhanced the cytoplasmic accumulation of viral RNA transcripts and the expression of viral proteins without significantly affecting the stability, splicing, or translation efficiency of the transcripts. Insertion of the CAE sequence also facilitated Rev-independent HIV Gag expression. We found that the CAE sequence interacted with NXF1, whereas disruption of NXF1 ablated CAE function. Thus, the CAE sequence mediates the cytoplasmic accumulation of gammaretroviral transcripts in an NXF1-dependent manner. Disruption of NXF1 expression impaired cytoplasmic accumulations of both spliced and unspliced RNA transcripts of XMRV and MLV, resulting in their nuclear retention or degradation. Thus, our results demonstrate that gammaretroviruses use NXF1 for the cytoplasmic accumulation of both spliced and nonspliced viral RNA transcripts.

IMPORTANCE

Murine leukemia virus (MLV) has been studied as one of the classic models of retrovirology. Although unspliced host messenger RNAs are rarely exported from the nucleus, MLV actively exports unspliced viral RNAs to the cytoplasm. Despite extensive studies, how MLV achieves this difficult task has remained a mystery. Here, we have studied the RNA export mechanism of MLV and found that (i) the genome contains a sequence which supports the efficient nuclear export of viral RNAs, (ii) the cellular factor NXF1 is involved in the nuclear export of both spliced and unspliced viral RNAs, and, finally, (iii) depletion of NXF1 results in nuclear retention or degradation of viral RNAs. Our study provides a novel insight into MLV nuclear export.

Although intron retention is a prominent form of alternative splicing in plants, it is rare in higher eukaryotes due to nonsense-mediated decay of intron-containing mRNA with premature stop codons (1). Retroviruses need to export both spliced and unspliced RNA transcripts from the nucleus to the cytoplasm (2, 3). Unspliced, intron-containing RNA transcripts are used as the templates for protein synthesis and as genomic RNA. Spliced RNA transcripts are used to produce viral Env. The splicing and nuclear export of retroviral transcripts are regulated by the cellular apparatus, which interacts with *cis*-acting sequences present within the viral genome and *trans*-acting viral regulatory proteins (4, 5). For example, human immunodeficiency virus type 1 (HIV-1) has a regulatory protein, Rev, which binds to the Rev response element (RRE) and interacts with a nucleocytoplasmic transport factor, CRM1 (chromosome region maintenance 1) (also known as exportin 1), to export intron-containing viral RNAs from the nucleus to the cytoplasm (6–8). Similarly, a complex betaretrovirus, mouse mammary tumor virus (MMTV), and a deltaretrovirus, human T cell leukemia virus (HTLV), encode the regulatory proteins Rem and Rex, which interact with *cis* elements in the viral transcripts to support nuclear export of unspliced viral transcripts through the CRM1 pathway (2, 6–12). Foamy viruses (spumaviruses) are unique in that they use a cellular RNA-binding protein, HuR, but not a viral regulatory protein to support nuclear export of unspliced viral transcripts through the CRM1 pathway (13).

Simple betaretroviruses, such as Mason-Pfizer monkey virus (MPMV), contain a *cis*-acting constitutive transport element (CTE), which binds directly to the nuclear export receptor NXF1 (nuclear RNA export factor 1) (also known as TAP) to mediate nuclear export of nonspliced viral RNA (14–16). Similarly, alpharetroviruses, such as avian sarcoma/leukemia viruses, have one or two copies of CTEs, which facilitate nuclear export of unspliced viral transcripts (17, 18). Overexpression of a dominant negative NXF1 mutant can modestly impair CTE-mediated gene expression (19). However, their CTEs lack any evident homology to the MPMV CTE (17). Furthermore, the Rous sarcoma virus CTE does not interact directly with NXF1 *in vitro* (18). Thus, it is possible that alpharetroviruses do not require the interaction of NXF1 with their CTEs for nuclear export of viral transcripts.

Although gammaretroviruses, such as amphotropic murine leukemia virus (AmphoMLV) 4070A or Moloney murine leukemia virus (MoMLV), have been extensively studied as model gam-

Received 4 December 2013 **Accepted** 18 January 2014

Published ahead of print 29 January 2014

Editor: S. R. Ross

Address correspondence to Yasuhiro Ikeda, ikeda.yasuhiro@mayo.edu.

Supplemental material for this article may be found at http://dx.doi.org/10.1128/JVI.03584-13.

doi:10.1128/JVI.03584-13

The authors have paid a fee to allow immediate free access to this article.

maretroviruses, their RNA export mechanisms are poorly understood. The gammaretrovirus proviral DNA consists of three main open reading frames (ORFs), *gag*, *pol*, and *env*, flanked by two long terminal repeats (LTRs), which are further divided into three regions, U3, R, and U5. The 5′ untranslated region (UTR) of viral RNA contains *cis*-acting elements essential for retroviral replication, including the primer-binding site (PBS), the major splice donor (SD), and the packaging signals. The Gag and Pol proteins are expressed from the unspliced transcripts. For expression of the viral glycoprotein Env, the Gag- and Pol-coding region is removed as an intron by a single splice event between the SD site and the splice acceptor (SA) site located upstream of the Env start codon. Previous studies have demonstrated that the sequences upstream of the 5′ major SD site determine the splicing efficiency of MLV transcripts (20, 21). However, the nuclear export pathway(s) and the mechanism controlling the cytoplasmic accumulation of viral transcripts remain elusive. Here, we demonstrate the use of NXF1 for the cytoplasmic accumulation of both spliced and unspliced gammaretroviral transcripts.

MATERIALS AND METHODS

Plasmid constructs. A plasmid encoding xenotropic murine leukemia virus (XMRV) Env (pX-Env) was described previously (22). The PCR primer set (pX-Env+CAE; see Table S1 in the supplemental material) was designed to amplify the target region of pXMRV. The resulting PCR fragment was inserted into pUb6. For the generation of HIV-1 Gag-expressing plasmid pHG, the HIV-1 *gag* ORF was PCR amplified using HIV-1 pNL4.3 as a template and inserted into the BamHI and EcoRI sites of pcDNA3.1(+) (Invitrogen). The RRE sequence from HIV-1 NL4.3, the CAE from pcDNA3.1(−)/XMRV, the AM-MLV CAE-like sequence from pAMS (AM is a fusion of amphotropic virus 4070A *pol-env* with the MoMLV *gag* region) (23), and the RD114 CAE-like sequence from pFB-RD-LF were amplified by using specific primers listed in Table S1 in the supplemental material and inserted into the EcoRI and NotI sites of pHG. Similarly, HIV-1 Gag expression plasmids with shorter CAE regions, including pHG+CAE(1-70), pHG+CAE(33-113), and pHG+CAE(77-146), were generated. All the deletion mutants of CAE in pHG-CAE were generated by using the QuikChange II site-directed mutagenesis kit (Stratagene) and oligonucleotides listed in Table S1 in the supplemental material. For the expression of a small interfering RNA (siRNA)-resistant NXF1 mutant, three silent mutations (AGAATCTCGATC [siRNA escape mutant]; nucleotides subjected to mutagenesis are underlined) were introduced into the siRNA-targeted region (AGGATATCTATC [wild type {WT}]) of pCMV-SPORT6-NXF1 (Open Biosystems). The ORFs of WT NXF1 or the escape mutants of NXF1 were then inserted into a lentiviral plasmid (pHRSINCSGW_PGRPuro) to create stably NXF1-expressing cells.

Cell lines and transfection. 293T and TE671 cells were cultured in Dulbecco's modified Eagle's medium with 10% fetal bovine serum at 37°C with 5% CO_2. Persistently XMRV-producing 22Rv1 cells were purchased from the ATCC. Persistently AM-MLV-infected TE671 cells were established through infection with culture supernatants of AM-MLV (pAMS)-transfected cells. For Western blot analysis of HIV-1 Gag, 293T cells (2×10^5 cells/well) were plated onto 6-well plates. Eight hours later, 1.0 μg of plasmid was transfected with FuGENE6 (Promega), and cells were harvested at 60 h posttransfection. For the mRNA stability assay, 2×10^5 293T cells were transfected with 0.5 μg of pX-Env or pX-Env+CAE; treated with a transcriptional inhibitor, actinomycin D (10 μg/ml; Sigma); and harvested at the indicated time points. Total cellular RNA samples were collected by using the RNeasy Plus kit (Qiagen) for reverse transcription quantitative PCR (RT-qPCR) analysis. For siRNA transfection, DharmaFECT transfection reagent (Dharmacon) was used according to the manufacturer's instructions. ON-TARGETplus nontargeting siRNA (Thermo Scientific) was used for the siRNA control. siRNAs used in this study are summarized in Table S1 in the supplemental material. For the generation of stably NXF1-expressing cell lines, AM-MLV-infected TE671 cells were transduced with the lentiviral vectors encoding wild-type NXF1 or the NXF1 escape mutant, and transduced cells were selected in the presence of puromycin. NXF1 overexpression was confirmed by Western blotting.

***In vitro* translation.** First, template DNA was produced by cloning XMRV Env (X-Env) or XMRV Env with a cytoplasmic accumulation element (X-Env+CAE) into the TOPO vector (Invitrogen). Template DNA was then linearized by HindIII before generating capped RNA by *in vitro* transcription according to the manufacturer's protocol (Promega). 293T cells were transfected with 0.5 μg of RNA with TransIT-mRNA reagent (Mirus). At 48 h posttransfection, nuclear and cytoplasmic cell lysates were harvested by using a Paris kit (Ambion), and protein expression was analyzed by Western blotting.

RNA pulldown assay. An RNA pulldown assay was performed as described previously by Tsai et al. (24), with modifications. Briefly, 60-nucleotide (nt) biotin-conjugated CAE RNAs from XMRV and MLV as well as 20 nt of unlabeled competitor RNA (see Table S1 in the supplemental material) were purchased from IDT. For each reaction, 5 nM the biotin-conjugated RNA and 500 nM the competitor RNA were used. They were first heated at 90°C for 2 min and then kept on ice for 2 min. After the addition of RNA structure buffer (10 mM Tris [pH 7], 0.1 M KCl, 10 mM $MgCl_2$), the RNAs were incubated at room temperature for 20 min to form proper secondary structures. Cytoplasmic and nuclear fractions were prepared by using the Paris kit (Ambion). Folded RNAs were mixed with 1 mg of 293T cell lysate and incubated at room temperature for 1 h. Dynabeads M-270 streptavidin (STA) (Invitrogen) was then added to each reaction mixture and incubated at room temperature for 1 h. Beads were washed five times with 1× wash buffer (2× wash buffer is 10 mM Tris-HCl [pH 7.5], 1 mM EDTA, and 2.0 M NaCl) and subjected to SDS-PAGE. Rabbit anti-NXF1 antibody (Sigma) and rabbit anti-exportin 1/Crm1 (Sigma) were used for Western blot analysis.

Western blotting. Protein samples in Laemmli sample buffer supplemented with β-mercaptoethanol were boiled at 95°C for 5 min, subjected to 4 to 15% SDS-PAGE (Bio-Rad), and transferred onto a polyvinylidene difluoride membrane. Membranes were blocked in 5% milk–phosphate-buffered saline–0.2% Tween 20 and stained with primary and secondary antibodies (rabbit anti-CSE1L [Novus], rabbit anti-importin 13 [Novus], mouse anti-β-actin [Sigma], mouse anti-glyceraldehyde-3-phosphate dehydrogenase [GAPDH] [Sigma], goat anti-MLV [ATCC], mouse anti-14-3-3σ [E-11] [Santa Cruz Biotech], rabbit anti-eIF1A [Abcam], and sheep anti-human importin alpha 2/KPNA2 [R&D]), followed by chemiluminescent detection using the ECL Western blotting substrate (Pierce). Protein expression was quantified by densitometric analysis (http://rsbweb.nih.gov/ij/) according to ImageJ guidelines. Student's *t* test was performed for statistical analysis.

RT-qPCR. Nuclear and cytoplasmic RNA samples were extracted by using a Paris kit (Ambion) according to the manufacturer's protocol. The RNA concentrations were determined by using a NanoDrop spectrophotometer (Thermo Scientific), and cDNA was synthesized by using RNA-to-cDNA EcoDry Premix (Clontech). The real-time qPCR assay was performed as described previously (25, 26).

Northern blotting. Probes were generated by using a North2South Random Prime DNA biotinylation kit (Pierce). The primers are listed in Table S1 in the supplemental material. Two to five micrograms of cytoplasmic and nuclear RNA samples was mixed with 10 μl deionized formamide (Millipore), 4.0 μl formaldehyde (Fisher Scientific), 2.0 μl of 10× morpholinepropanesulfonic acid (MOPS) buffer (Fisher Scientific), 2.0 μl of 0.4 mg/ml ethidium bromide, and 1.0 μl of 0.2% bromophenol blue dye mix (0.2% bromophenol blue, 10 mM EDTA, and 50% glycerol in diethyl pyrocarbonate [DEPC]-treated water). RNAs were heated at 65°C for 10 min before loading onto a 1.2% formaldehyde agarose gel. After electrophoresis, the gels were rinsed with autoclaved water for 15 min and immersed in autoclaved 20× SSC (1× SSC is 0.15 M NaCl plus 0.015 M

sodium citrate) for 1 h with gentle shaking. RNA was then transferred onto nylon membranes (Pierce) overnight and fixed by UV cross-linking. Probe hybridization and signal detection were performed according to the protocol provided with the North2South chemiluminescent hybridization and detection kit (Pierce).

RNA sequencing (RNA-Seq). Nuclear and cytoplasmic RNAs were isolated from MLV-infected TE671 or pXMRV-transfected 293T cells 2 days after transfection of the NXF1 siRNA or a control siRNA. The processing of the mRNA data was performed by using MAP-RSeq v. 1.2.1. MAP-RSeq consists of the following steps: alignment, quality control, obtaining genomic features per sample, and, finally, summarizing the data across samples. The pipeline provides detailed quality control data to estimate the distance between paired-end reads, evaluate the sequencing depth for alternate splicing analysis, determine the rate of duplicate reads, and evaluate the coverage of reads across genes using RSeQC v 2.3.2 software (27). Paired-end reads were aligned with TopHat 2.0.6 (28) against the hg19 genome build by using the bowtie1 aligner option (29). Gene counts were generated by using HTseq software (http://www-huber.embl.de/users/anders/HTSeq/doc/overview.html), and gene annotation files were obtained from Illumina (http://cufflinks.cbcb.umd.edu/igenomes.html). Paired-end reads were also mapped to the MLV sequence (GenBank accession number AF010170.1) by using BWA (30), and coverage across the viral genes was calculated by using GATK DiagnoseTargets v 2.4-3 (31). Differential expression analysis was performed by using edgeR v.2.6.2 (32), using triplicates for each group analyzed. The gene expression of viral reads obtained from cells treated with siRNA targeting NXF1 was normalized to the read counts obtained from cells treated with the siRNA control. Increases and decreases in the viral gene expression level were indicated as percentages. The false discovery rate (FDR) was fixed to 0.1, and significant changes ($n = 3$) in viral gene expression levels between control and NXF1-specific siRNAs, or with overexpression of an NXF1 escape mutant, were determined.

RNA immunoprecipitation. Nuclear lysate was isolated from TE671 cells infected with MLV by using buffers supplied with the Paris kit (Ambion). Chromatin was sheared by passing through a syringe needle five times, and the nuclear membrane and debris were pelleted by centrifugation at 13,000 rpm for 10 min. Antibody (5 μg) was added to 10 mg of supernatant and incubated for 2 h at 4°C. Protein A-Sepharose CL-4B (GE Healthcare) was then added to the mixture, and the mixture was incubated again for 1 h at 4°C. Sepharose beads were pelleted at 2,500 × *g* for 30 s and washed with RNA immunoprecipitation (RIP) buffer (150 mM KCl, 25 mM Tris [pH 7.4], 5 mM EDTA, 0.5 mM dithiothreitol [DTT], 0.5% NP-40, 100 U/ml RNase inhibitor, and protease inhibitor) five times, followed by one wash in phosphate-buffered saline. RNA was extracted by using the RNeasy Plus minikit (Qiagen), and cDNA was synthesized (Clontech) for PCR. Primers for RIP are listed in Table S1 in the supplemental material as RIP AM-MLV *gag* and RIP AM-MLV *env*.

RESULTS

Identification of a novel *cis*-acting element facilitating efficient XMRV Env expression. It is known that the expression of MLV envelope proteins from heterologous vectors is inefficient. We found this to be the case with the xenotropic MLV XMRV (22). Insertion of the 146-nt sequence termed the CAE (cytoplasmic accumulation element) (Fig. 1A), which is at the end of the *pol* gene, strongly enhanced the expression of Env to levels comparable to that of an infectious molecular clone, pXMRV (Fig. 1B). In this 146-nt CAE sequence, we found an in-frame CTG codon, upstream of the putative XMRV Env starting ATG codon, as well as the splice acceptor site for the *env* transcripts. Several retrovirus proteins, such as MLV glycosylated Gag and equine infectious anemia virus (EIAV) Tat, are translated from a CTG initiation codon (33, 34). To rule out a possible role of the in-frame CTG site in the CAE-mediated increase in the XMRV Env expression level, we introduced mutations into the CTG site (pX-Env+CAEΔCTG) or the putative ATG start codon (pX-Env+CAEΔATG). We also generated a mutant with a disruption in the splice acceptor site (pX-Env+CAEΔSA). Our data showed no involvement of CTG and the splice acceptor sites in CAE function (Fig. 1B). In addition, the use of the CAE-containing XMRV Env expression construct also increased XMRV Env-pseudotyped gammaretroviral and lentiviral vector titers (Fig. 1C).

The CAE mediates the cytoplasmic accumulation of XMRV *env* transcripts without affecting the splicing, stability, or translational efficiency of viral transcripts. To assess the potential effect of the CAE insertion on the splicing of viral transcripts, we harvested cytoplasmic RNAs from 293T cells transfected with pX-Env or pX-Env+CAE and analyzed the splicing patterns of the *env* transcripts by Northern blotting. Although the introduction of the 146-nt CAE sequence increased the level of *env* transcripts, no notable change in the splicing patterns of *env* was observed (Fig. 2A). We then assessed the influence of the CAE addition on the stability of the viral transcripts. Actinomycin D-mediated pulse-chase stability assays demonstrated that the mRNA half-life was estimated to be 12.0 or 13.95 h in the absence or presence of the CAE sequence, respectively, which was not statistically significant (Fig. 2B). We also found that the introduction of the CAE had no effect on the stability of viral transcripts when mRNAs were transcribed *in vitro* (data not shown). To assess the influence of the CAE addition on the translation of viral transcripts, the *in vitro*-transcribed *env* mRNAs were transfected into 293T cells, and the levels of XMRV Env expression were assessed by Western blotting. As shown in Fig. 2C, the CAE had no effect on translational efficiency. Finally, we compared the abundances of nuclear and cytoplasmic *env* transcripts between the two constructs. The insertion of the CAE sequence did not affect the nuclear levels of viral transcripts but increased the cytoplasmic levels of Env-encoding transcripts approximately 15-fold at 8 h posttransfection (Fig. 2D). These data demonstrated that the CAE sequence contains a *cis*-acting element that enhances the cytoplasmic accumulation of viral transcripts without affecting their splicing, stability, or translational efficiency.

The CAE sequence supports Rev-independent expression of HIV-1 Gag. To confirm the putative nuclear export activity, we introduced the XMRV CAE sequence into a Rev-dependent HIV Gag expression construct, pHG (Fig. 3A). As expected, Rev-independent HIV Gag expression was inefficient in the absence of Rev, but remarkably, insertion of the CAE sequence significantly increased Gag expression levels in a Rev-independent manner (Fig. 3B). *trans*-complementation by Rev transfection increased the Rev/RRE-dependent Gag expression level but not the CAE-mediated Gag expression level (Fig. 3B). Our data therefore suggest that the CAE can compensate for Rev/RRE-mediated nuclear export of HIV transcripts. Deletion analysis of CAE showed that the insertion of the first 70 nt, pHG+CAE(1-70), mediated a similar enhancement (Fig. 3C).

Further mapping identified an essential 9-nt core CAE region, which is highly conserved among gammaretroviruses. Related gammaretroviruses, including MLV strains, gibbon ape leukemia virus, feline leukemia virus, and feline endogenous virus RD114, have conserved CAE-like sequences (70 nt) (Fig. 4A). The introduction of the CAE-like sequences from amphotropic MLV or RD114 also rescued Rev-independent HIV Gag expression (Fig. 4B). To further map the region essential for CAE activity, we gen-

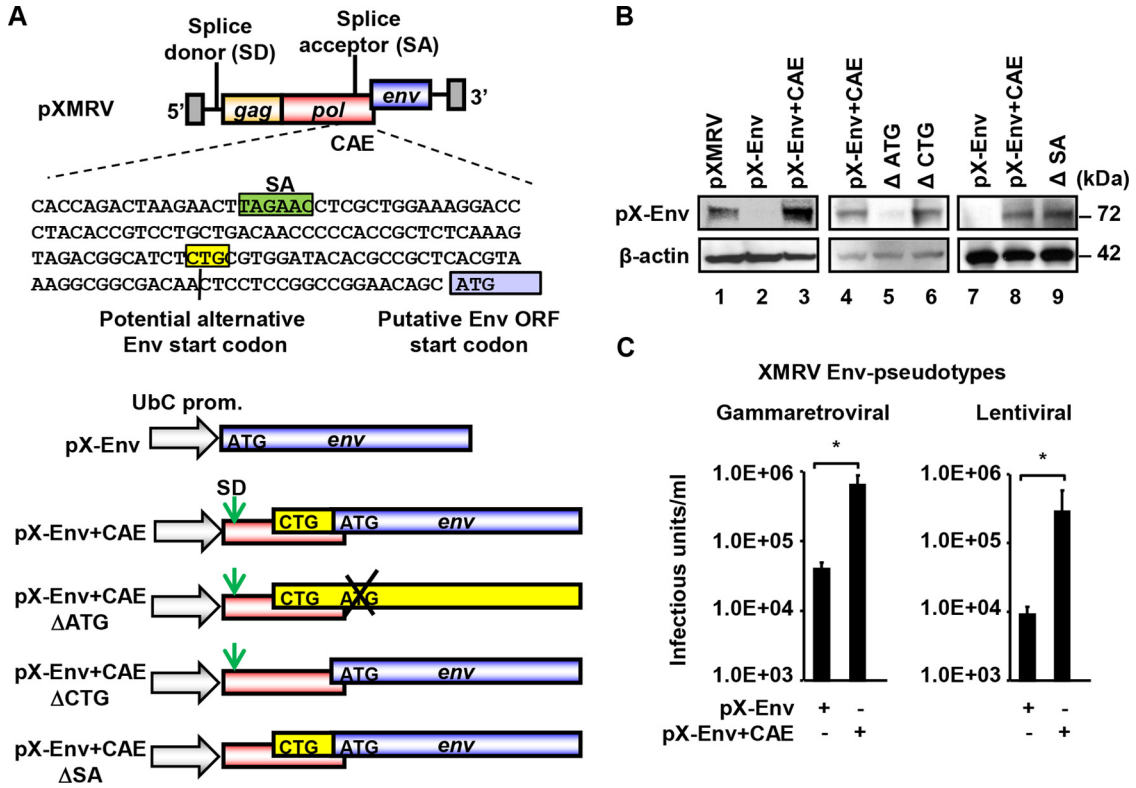

FIG 1 Identification of a *cis*-acting element, CAE, in the *pol* gene of XMRV. (A) Schematic representation of plasmids encoding the XMRV Env ORF alone (pX-Env), the XMRV Env ORF with an additional CAE (pX-Env+CAE), and deletion mutants (ΔATG, ΔCTG, or ΔSA) of pX-Env+CAE. Plasmids are based on pUB6, and Env expression is driven by the UbC promoter, as shown by the arrows. Potential known *cis* elements in the CAE sequence, including the splice acceptor for the *env* transcript and an in-frame upstream CTG codon, along with the putative Env start codon ATG, are indicated in boxes. (B) Western blot analysis was performed to detect XMRV Env expression of pX-Env, pX-Env+CAE, and pX-Env+CAE with deletions in the SA, CTG, or ATG site. An infectious clone of XMRV (pXMRV) was included as a control. β-Actin was also detected as a loading control. (C) Flow cytometry was performed to determine the infectious titers of the green fluorescent protein-expressing MLV- and HIV-1-based vectors. XMRV Env-pseudotyped gammaretroviral and lentiviral vectors were made in 293T cells transfected with pX-Env or pX-Env+CAE. Error bars represent standard deviations from three independent experiments, with statistical significance determined by a two-tailed Student *t* test (∗, $P < 0.05$).

erated a series of deletion mutants based on the pHG-CAE(1-70) construct (pHG-CAEΔ1, -Δ2, -Δ3, and -Δ4) (Fig. 4A). Introduction of the deletion into the highly conserved region (pHG-CAEΔ2) abolished CAE function (Fig. 4C).

RNA secondary structure is essential for posttranscriptional control for simian retrovirus (35, 36) and recruits cellular proteins for nuclear export of the transcripts (16). RNAfold software (http://rna.tbi.univie.ac.at/cgi-bin/RNAfold.cgi) was therefore used to predict two potential forms of the CAE sequences with stem-loop structures (Fig. 4D). Based on the predictions, we generated pHG+CAE-based mutants with deletions in the stem or the whole loop regions (Fig. 4D). As shown in Fig. 4E, deletion of the individual stem or loop sequences did not affect CAE function. Based on these results, we tested a pHG+CAE mutant with a deletion in the conserved GGAAAGGAC sequence, which demonstrated that the 9-nt GGAAAGGAC sequence was essential for CAE activity (Fig. 4F). The introduction of the GGAAAGGAC sequence alone failed to rescue HIV-1 Gag expression, indicating that this sequence is essential but not sufficient to mediate Rev-independent HIV-1 Gag expression (Fig. 4F).

NXF1 is required for CAE-mediated cytoplasmic accumulation of viral transcripts and expression of the viral Env protein. We reasoned that the CAE interacts with a nuclear export factor to facilitate efficient cytoplasmic accumulation of viral transcripts. Our attempts to identify CAE-interacting host factors by pulling down the biotin-labeled CAE sequence yielded several candidate proteins. However, disruption of these proteins failed to reduce CAE function (not shown). We therefore assessed the effects of inhibiting major importin/karyopherin-β family proteins (37–49) on CAE function. We first tested the effect of leptomycin B (LMB), which inhibits nuclear export through the CRM1 pathway. As expected, LMB treatment strongly reduced the expression of Rev-dependent HIV-1 Gag (Fig. 5A). In contrast, LMB did not affect the expression of the XMRV Env and Gag proteins (Fig. 5B).

For screening of major importin/karyopherins and the major nucleocytoplasmic transport receptor NXF1, we used specific siRNAs. To minimize indirect effects induced by sustained ablation of individual nuclear export pathways, we assessed the effects of siRNA treatments 48 h after siRNA transfection. We first assessed functional controls for the downregulated karyopherins. Disruption of CRM1 (XPO1), NXF1, exportin 7 (XPO7), importin 13 (IPO13), and exportin 2 (XPO2) reduced Rev-dependent HIV-1 Gag expression (Fig. 5C), MPMV CTE-mediated HIV-1 Gag expression (Fig. 5D), nuclear export of 14-3-3δ (Fig. 5E), nuclear import of eIF1A (Fig. 5F), and nuclear export of IPO-α (Fig. 5G), respectively. We then examined the effects of ablation of

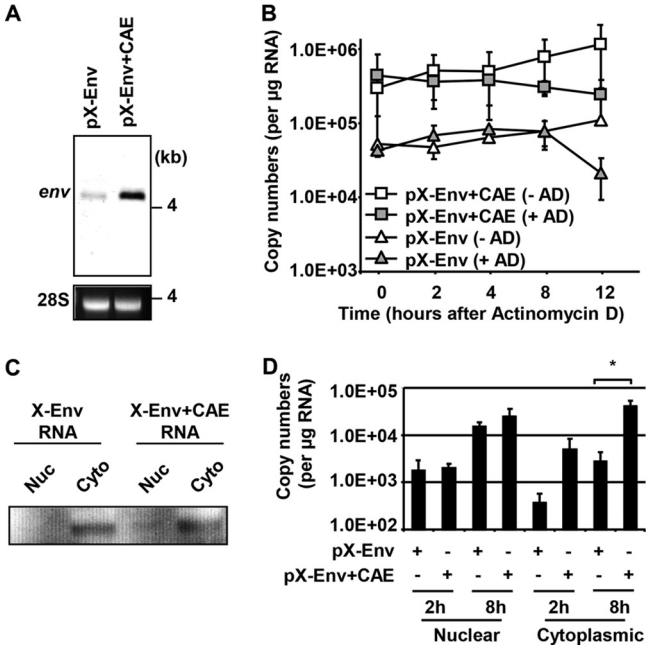

FIG 2 The CAE mediates the cytoplasmic accumulation of viral transcripts. (A) Northern blotting was performed to detect *env* transcripts from the two XMRV Env expression plasmids (pX-Env and pX-Env+CAE). 293T cells were transfected with pX-Env or pX-Env+CAE. The cytoplasmic fraction of RNA was used for analysis. Ethidium bromide staining of cytoplasmic rRNA (28S) is shown as a loading control. (B) A pulse-chase assay was performed to assess the stability of the *env* transcripts with or without the CAE. Total RNAs were harvested at 2, 4, 8, and 12 h posttransfection after treatment with actinomycin D (+AD) (in dimethyl sulfoxide) or dimethyl sulfoxide. The levels of viral transcripts in RNA samples were determined by RT-qPCR using a specific primer-and-probe set for the XMRV *env* sequence. Error bars represent standard deviations of three independent experiments. (C) To assess the influence of the CAE on translation efficiency, 293T cells were transfected with an equivalent amount of X-Env RNA or X-Env+CAE RNA, which was synthesized by *in vitro* transcription. Western blot analysis was performed to determine the levels of XMRV Env expression. (D) RT-qPCR analysis was performed to determine the copy numbers of *env* transcripts in the nucleus and the cytoplasm. pX-Env or pX-Env+CAE was transfected into 293T cells. RNA samples from the nuclear and cytoplasmic fractions were analyzed at 2 and 8 h posttransfection. + and − indicate the presence and absence of the plasmid, respectively. Error bars represent standard deviations from three independent experiments, with statistical significance determined by a two-tailed Student *t* test (∗, $P < 0.05$).

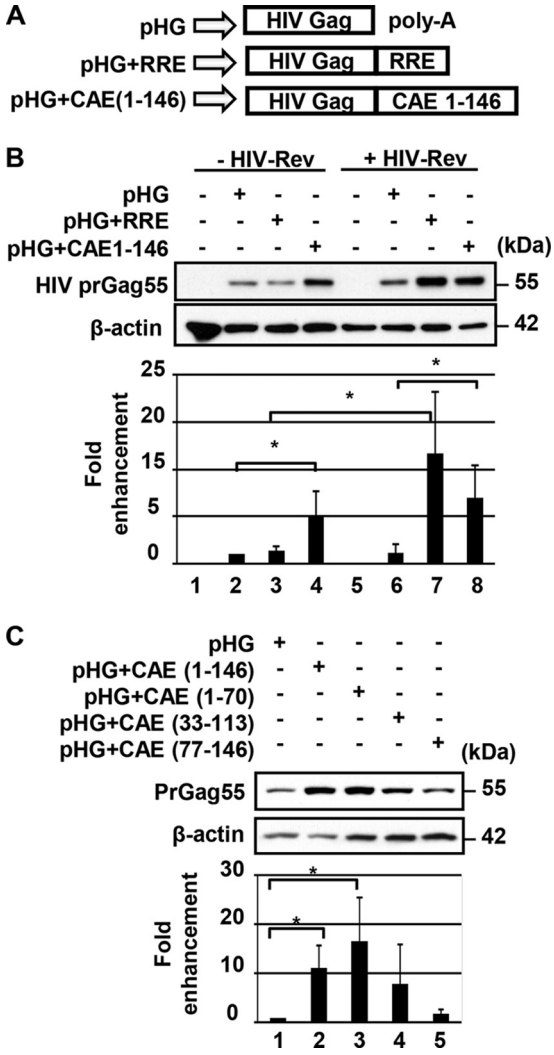

FIG 3 The CAE sequence supports Rev-independent expression of HIV-1 Gag. (A) Schematic representation of Rev-dependent HIV-1 Gag expression construct pHG and its derivatives with the 858-nt RRE (pHG+RRE) or the full-length 146-nt CAE [pHG+CAE(1-146)]. (B) 293T cells were transfected with pHG, pHG+RRE, or pHG+CAE, with or without a Rev expression plasmid (0.2 μg), and Rev-independent and Rev-dependent HIV-1 Gag expression was assessed by Western blotting using mouse anti-HIV antibody. (C) A series of CAE deletion mutants was compared with pHG and pHG+CAE(1-146) for their ability to rescue Rev-independent HIV-1 Gag expression. Deletion mutants of the CAE region are indicated as follows: 1-146 contains 146 nt of the CAE, as indicated above for panel A; 1-70 contains the first 70 nt of the CAE from the 5′ end; 33-113 contains the middle portion of the CAE (81 nt); and 77-146 contains the 70 nt of the CAE from the 3′ end. These plasmids were transfected into 293T cells. (B and C) Relative band density normalized to the HIV-1 Gag signal, with pHG set to 1. Error bars represent standard deviations from three independent experiments, with statistical significance determined by a two-tailed Student *t* test (∗, $P < 0.05$).

CRM1 (XPO1), XPO2, IPO13, NXF1, and XPO7 expression on CAE-mediated XMRV Env expression. As shown in Fig. 5H, only NXF1 knockdown impaired Env expression in pX-Env+CAE-transfected 293T cells and in persistently XMRV-infected 22Rv1 cells. No notable effect was observed with the other siRNA treatments. Silencing of XPOT, XPO4, XPO5, and XPO6 expression showed no effect on CAE-mediated XMRV Env expression (data not shown). Real-time PCR analysis further revealed that NXF1 depletion significantly decreased the cytoplasmic levels of *env* transcripts of pX-Env+CAE but not those of pX-Env (Fig. 5I), which suggested the involvement of NXF1 in the CAE-mediated nuclear export of XMRV *env* transcripts.

To assess the interaction between NXF1 and the CAE sequence, we performed an RNA pulldown assay using a biotin-labeled, 60-nt XMRV CAE RNA sequence and streptavidin (STA) beads. Western blot analysis with anti-NXF1 antibody detected NXF1 in the XMRV CAE(1-60) pulldown with cell lysates (Fig. 5J). Another major receptor, CRM1, did not show an interaction with CAE (Fig. 5J), which is consistent with the results shown in Fig. 5B. Similar results were also observed when a biotin-labeled 60-nt CAE-like RNA from amphotropic MLV was used as a probe (Fig. 5K). The addition of unlabeled competitor RNA (20-nt sequence from the Δ2 region) (Fig. 4A) containing the 9-nt CAE core sequence (GGAAAGGAC) strongly prevented NXF1 pulldown by a

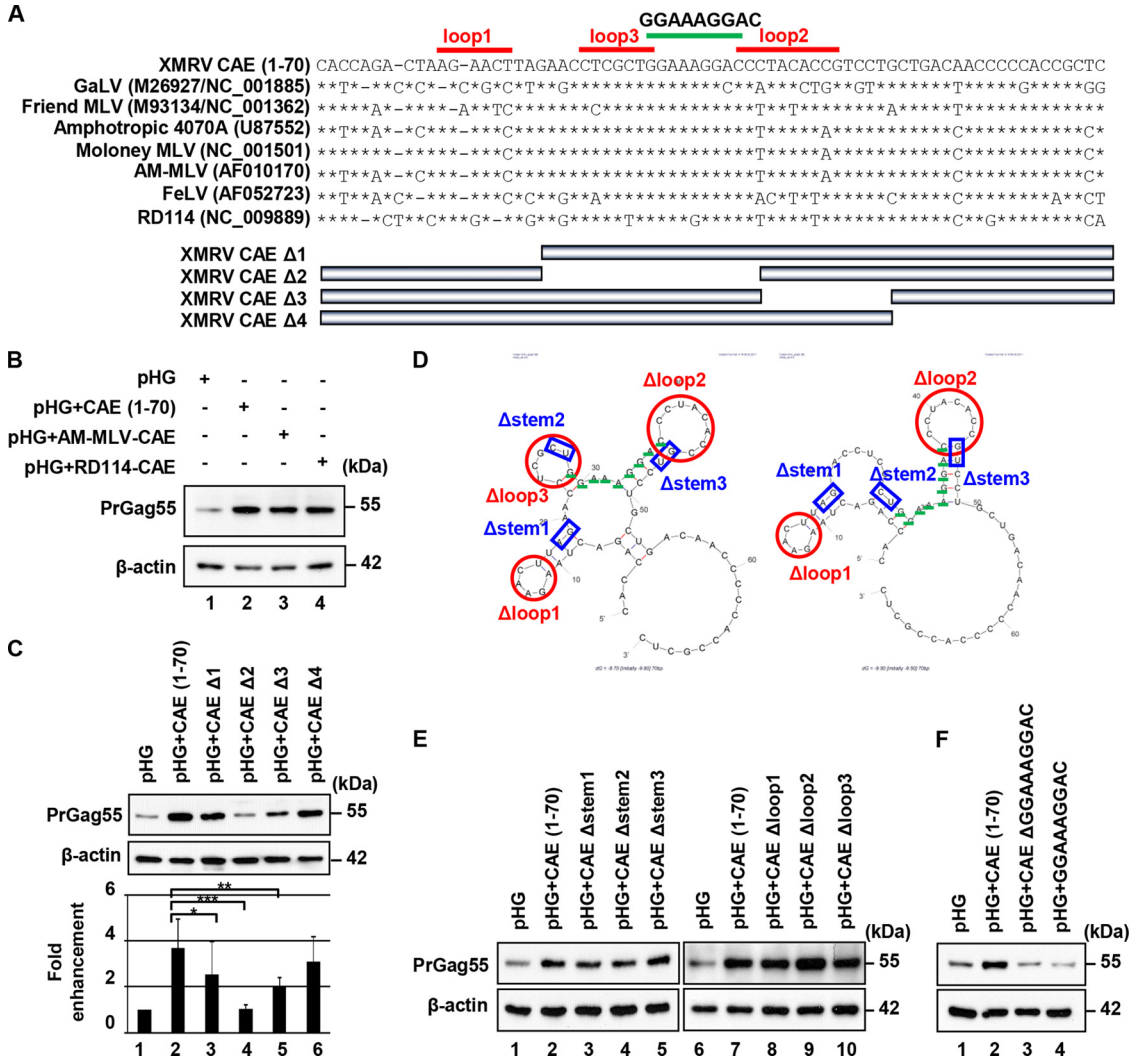

FIG 4 Mapping analysis of the 70-nt CAE. (A) Gammaretroviral CAE-like sequences were aligned to the CAE of XMRV. Series of deletion mutants (CAEΔ1 to CAEΔ4) are also indicated at the bottom. Gray bars correspond to the XMRV CAE sequences inserted into the pHG plasmid. GenBank accession numbers are indicated in parentheses. GaLV, gibbon ape leukemia virus; FeLV, feline leukemia virus. (B) CAE-like sequences (70 nt) from MLV and RD114 were inserted into pHG, and the effect on HIV-1 Gag expression was compared to those of pHG and pHG+CAE(1-70) by Western blotting. (C) Western blotting was performed to determine Rev-independent HIV-1 Gag expression by pHG-CAE(1-70)-derived deletion mutants (CAEΔ1 to CAEΔ4, shown in panel A). 293T cells were transfected with the indicated plasmids. The relative band density was normalized to the HIV-1 Gag signal, with pHG set to 1. Error bars represent standard deviations from three independent experiments, with statistical significance determined by a two-tailed Student *t* test (*, $P < 0.05$; **, $P < 0.01$; ***, $P < 0.001$). (D) RNAfold software (http://rna.tbi.univie.ac.at/cgi-bin/RNAfold.cgi) was used to predict two potential secondary structures of the CAE sequence. The indicated stem regions (blue) or loop regions (red) were mutated or deleted, respectively. Loop regions 1 to 3 are also indicated in panel A. (E) Western blotting was performed to determine Rev-independent HIV-1 Gag expression by the pHG+CAE(1-70)-derived mutants (Δstem1 to -3 and Δloop1 to -3). 293T cells were transfected with the indicated plasmids, and the HIV Gag expression level was compared with that of pHG+CAE(1-70). β-Actin was stained as a loading control. (F) Western blotting of HIV-1 Gag expression with a 9-nt deletion or the insertion of the 9-nt minimum sequence (+GGAAAGGAC). β-Actin was detected as a loading control. The minimum sequences are also indicated in panels A and D (green).

biotin-labeled CAE sequence (Fig. 5L). These observations confirmed the interaction between NXF1 and gammaretroviral CAE sequences and the importance of the 9-nt core sequence in this interaction.

NXF1 is required for efficient nuclear export of unspliced gammaretroviral transcripts. Short-term disruption of NXF1 expression did not strongly affect the levels of accumulated XMRV Gag polyproteins in persistently XMRV-infected 22Rv1 cells (Fig. 5H). However, we noted that disruption of NXF1 impaired the accumulation of XMRV Gag proteins in 293T cells transiently transfected with an infectious molecular clone of XMRV. Transfection of the NXF1 siRNA for 48 h significantly reduced the levels of Env and Gag p65 and p30 proteins without affecting the levels of endogenously expressed housekeeping genes (Fig. 6A). When quantified, transfection of the NXF1 siRNA reduced the levels of Gag and Env 3.3- and 67-fold, respectively ($n = 3$) ($P < 0.002$ and $P < 0.001$, respectively). Real-time RT-PCR analysis also demonstrated that NXF1 depletion resulted in significant nuclear accumulation and reduced cytoplasmic abundances of *pol* and *env* transcripts (Fig. 6B). These data indicate that NXF1 plays a critical role in the nuclear export of both spliced and unspliced viral transcripts.

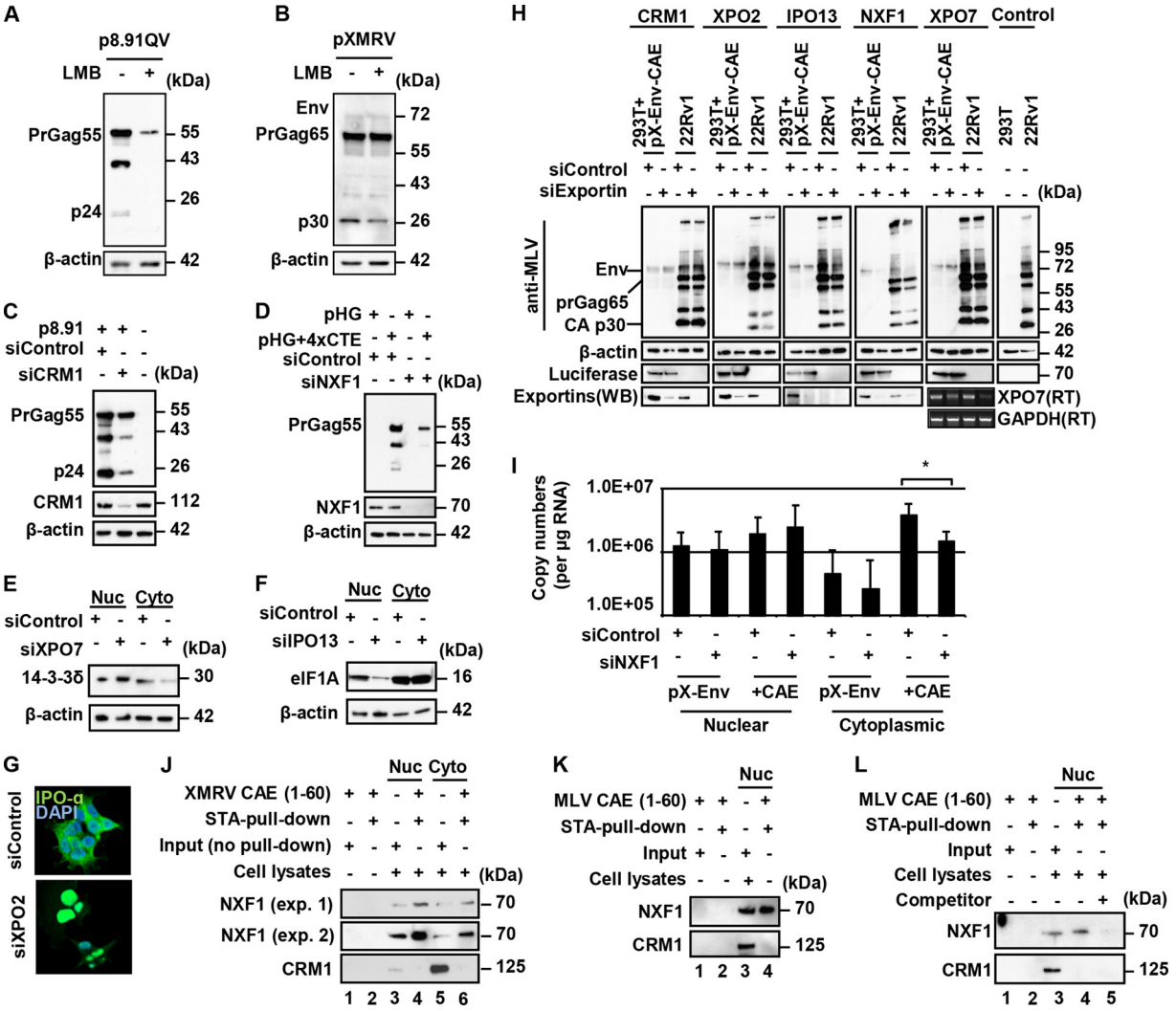

FIG 5 NXF1 is required for CAE-mediated cytoplasmic accumulation of viral transcripts. (A) 293T cells were transfected with p8.91QV (HIV Gag-, Pol-, Rev-, Tat-, and RRE-containing plasmid). At 18 h posttransfection, cells were treated with leptomycin B (0 nM [−] or 20 nM [+], as indicated). At 24 h post-drug treatment, cells were harvested and subjected to Western blotting. (B) Same as panel A except that an infectious clone of XMRV (pXMRV) was used. (C to G) Functional controls for siRNAs used to block individual nuclear export pathways. (C) 293T cells were transfected with the indicated siRNAs and p8.91QV. Western blot analysis was performed to determine the expression levels of XPO1/CRM1 and CRM1- and Rev-dependent HIV Gag proteins. (D) Four copies of the MPMV CTE element were inserted into the pHG construct, resulting in pHG+4×CTE, as described previously by Swanson et al. (15). Western blotting was performed to verify the effects of NXF1-targeting siRNA on NXF1 expression and NXF1- and CTE-dependent HIV-1 Gag expression. (E to G) At 48 h posttransfection, the effects of siRNA-mediated disruption of XPO7, IPO13, and XPO2 (38, 39, 49) on the transport of known target proteins (14-3-3δ, eIF1A, and IPO-α) were analyzed by either Western blotting (E and F) or immunohistochemistry (G) (71). DAPI, 4′,6-diamidino-2-phenylindole. (H) Effects of depletion of the indicated karyopherin-β protein family or NXF1 on expression of XMRV proteins were analyzed by Western blotting (WB). 293T cells were transfected with siRNAs, followed by cotransfection with 0.4 μg of pX-Env+CAE and 0.2 μg of a plasmid expressing luciferase (as a transfection/toxicity control). Cells were harvested 48 h after siRNA transfection. Persistently XMRV-infected 22Rv1 cells were transfected with siRNAs and harvested 48 h later. Western blotting was performed by using goat anti-MLV antibody, mouse anti-β-actin as a loading control, and specific antibodies for the nuclear export proteins. Silencing of XPO7 was verified by RT-PCR, with GAPDH as a control. (I) Influence of NXF1 knockdown on the nuclear export of XMRV *env* transcripts. 293T cells were transfected with pX-Env and pX-Env+CAE (indicated as +CAE) as well as the indicated siRNAs. RT-qPCR was performed to quantify the levels of XMRV *env* transcripts in the nucleus and the cytoplasm. (J to L) Interaction of NXF1 and the CAE sequence was determined by an RNA pulldown assay. Nuclear (Nuc) or cytoplasmic (Cyto) cell extracts from TE671 cells were incubated with the biotin-labeled XMRV (J) or MLV (K and L) CAE RNA in the presence of competitor RNA (lane 5 in panel L). The CAE RNA was pulled down with streptavidin (STA)-conjugated magnetic beads, followed by Western blotting of copurified proteins using anti-NXF1 or anti-CRM1 antibody. The presence or absence of the biotin-conjugated CAE RNA, streptavidin, cell lysate, and unconjugated competitor RNA is shown as + or −, respectively.

XMRV is recombinant between endogenous polytropic and xenotropic MLVs (50). To examine whether other mouse gammaretroviruses utilize a similar mechanism of RNA export, we examined the behavior of a chimeric AM-MLV, pAMS (ATCC 45167) (23). This virus has an amphotropic 4070A *env* gene in a Moloney MLV background, allowing AM-MLV replication in human cells. As shown in Fig. 6C, immunoprecipitation of NXF1 in persistently AM-MLV-infected TE671 cells, followed by RT-PCR, detected both spliced and unspliced MLV transcripts, suggesting an interaction of NXF1 with unspliced MLV tran-

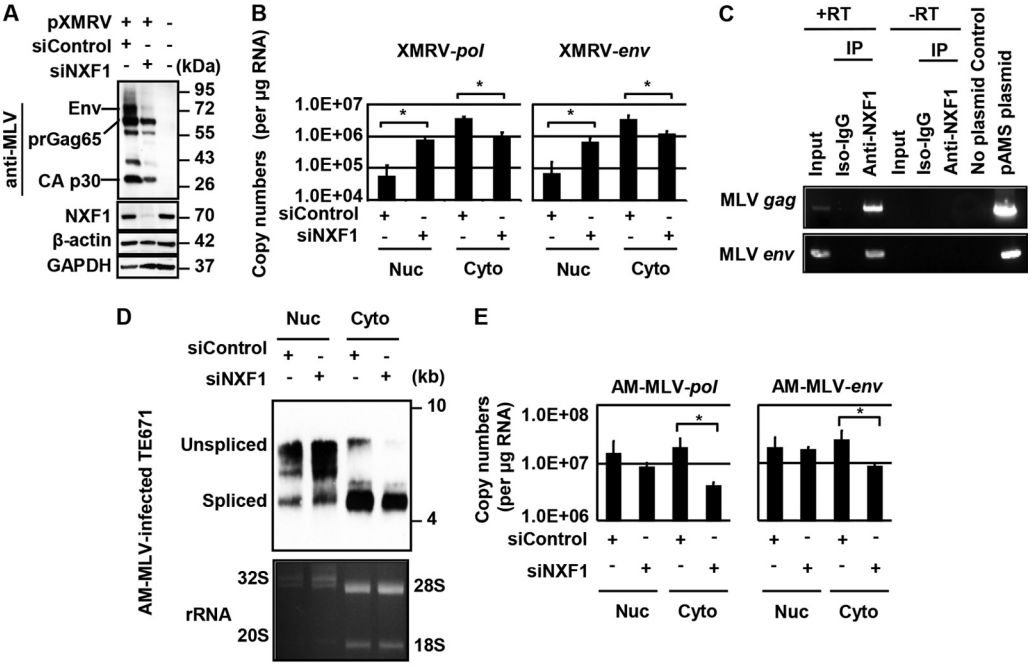

FIG 6 Gammaretroviruses require NXF1 for nuclear export of viral transcripts. (A) 293T cells were transfected with the indicated siRNAs, followed by transfection with 0.4 μg of pXMRV. Cells were harvested 48 h after siRNA transfection for protein expression analysis. Viral Gag and Env proteins were detected by anti-MLV antibodies. As loading controls, β-actin and GAPDH were also detected by specific antibodies. (B) RT-qPCR was performed to quantify XMRV transcripts in the nucleus and the cytoplasm upon disruption of NXF1 expression. 293T cells were treated with the indicated siRNAs, and the specific primer-and-probe sets were used to determine the copy numbers of XMRV *pol* and *env* transcripts. Average viral RNA copy numbers (per μg of RNA) from three independent experiments are shown. Error bars represent standard deviations, with statistical significance indicated by ∗ ($P < 0.05$). (C) RIP assay to detect NXF1-associated viral transcripts. Anti-NXF1 antibody was used to immunoprecipitate NXF1 and associated transcripts from nuclear lysates of MLV-infected TE671 cells. RT-PCR was performed to detect MLV transcripts in RNA samples isolated from the immunoprecipitates. PCR was performed with samples after reverse transcriptase reactions (+RT) or without reverse transcriptase reactions (−RT), using MLV-specific primers. As a control, immunoprecipitation (IP) was also conducted in the presence of an isotype control antibody (Iso-IgG). Water (mock) and the pAMS MLV plasmid were also used as PCR controls. (D) Northern blot analysis was performed to determine the influence of the NXF1 disruption on viral transcripts in AM-MLV-infected TE671 cells. Nuclear and cytoplasmic RNA samples were harvested 48 h after transfection of control or NXF1-targeting siRNA. Ethidium bromide staining of the nuclear (32S and 20S) and cytoplasmic (28S and 18S) rRNAs is also shown as a loading control. (E) RT-qPCR was performed to quantify viral transcripts in the nucleus and the cytoplasm upon siRNA treatment of AM-MLV-infected TE671 cells. Average unspliced and spliced viral RNA copy numbers (per μg of RNA) from five independent experiments are shown. Error bars represent standard deviations (∗, $P < 0.05$ by a two-tailed Student *t* test).

scripts. Northern blot analysis demonstrated that siRNA-mediated NXF1 depletion for 48 h impaired the cytoplasmic accumulations of *env* and *gag* transcripts in AM-MLV-infected TE671 cells (Fig. 6D). Real-time PCR analysis also confirmed a significantly reduced cytoplasmic accumulation of spliced and unspliced MLV transcripts (Fig. 6E).

Minimal off-target or indirect effects of siRNA-mediated NXF1 depletion. To rule out potential off-target or toxic effects of the NXF1-specific siRNA, we generated a lentiviral vector expressing a siRNA-resistant NXF1 mutant, NXF1-Escape. We also generated a control lentivector expressing a wild-type NXF1 protein. Persistently AM-MLV-infected TE671 cells were stably transduced by the lentiviral vectors, resulting in cells overexpressing wild-type NXF1 or NXF1-Escape (AM-MLV-infected TE671+ NXF1-WT1 and -WT2 or -ESC1 and -ESC2, two biological replicates for the wild-type and NXF1-Escape constructs, respectively). Using these cells, we assessed the influence of NXF1 siRNA transfection. The introduction of the NXF1-Escape mutant, but not wild-type NXF1, resulted in the overexpression of siRNA-resistant NXF1, which rescued the defects in cytoplasmic accumulation of MLV transcripts upon depletion of NXF1 (Fig. 7A).

To assess the influence of siRNA-mediated NXF1 knockdown on viral and cellular transcripts, we also performed deep sequencing analysis of nuclear and cytoplasmic RNAs from AM-MLV-infected TE671 cells (AM-MLV-infected TE671 cells treated with the control siRNA or the NXF1 siRNA and AM-MLV-infected TE671 cells stably overexpressing NXF1-Escape; $n = 3$ per each treatment) (Fig. 7B). The NXF1 siRNA treatment demonstrated significantly reduced nuclear and cytoplasmic NXF1 transcript levels in AM-MLV-infected TE671 cells (75% reduction in cytoplasmic NXF1 transcripts) (Fig. 7B). NXF1 depletion also significantly reduced MLV *env* and *pol* transcript levels in the cytoplasm but not in the nucleus (Fig. 7B). Lentiviral overexpression of siRNA-resistant NXF1 achieved 7.8- and 17.5-fold increases in NXF1 transcript levels in the nucleus and the cytoplasm, respectively, which significantly increased viral sequence reads in the cytoplasm but not in the nucleus (Fig. 7B). These data further indicate that the cytoplasmic accumulation of spliced and unspliced MLV transcripts is regulated by the NXF1-mediated nuclear export pathway. Transfection of the NXF1 siRNA for 48 h did not significantly affect the nuclear and cytoplasmic levels of most cellular transcripts, including actin and GAPDH. These observations indicated minimal off-target or indirect effects of siRNA-mediated NXF1 depletion.

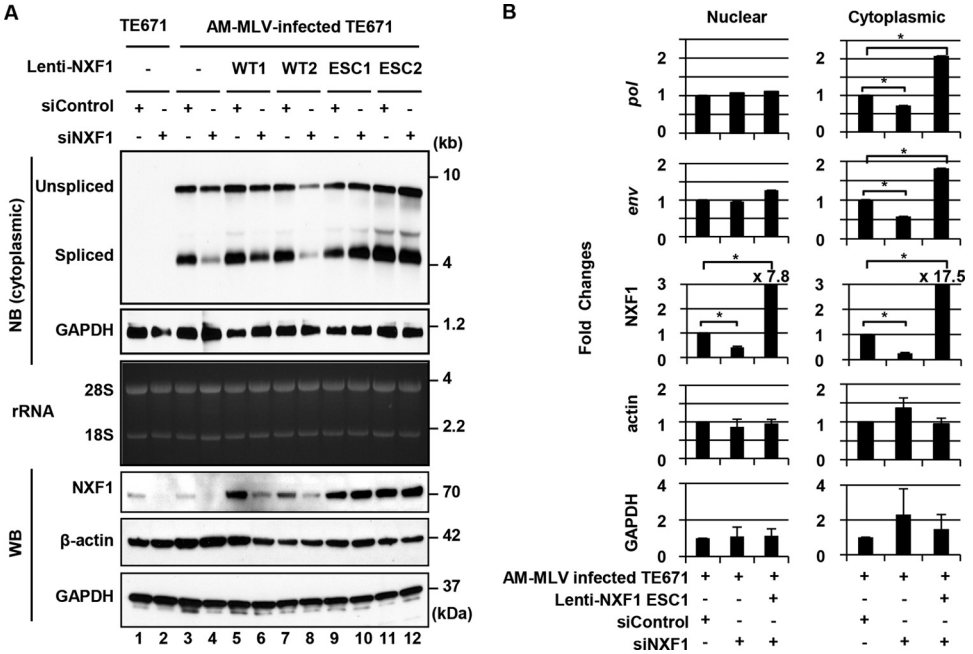

FIG 7 Influence of NXF1 depletion on nuclear export of MLV transcripts. (A) An siRNA rescue assay was performed to rule out off-target effects of siRNA. Northern blot (NB) analysis was performed to determine the effect of transfection of NXF1 siRNA on MLV transcripts in AM-MLV-infected TE671 cells with stable expression of wild-type NXF1 (WT1 or WT2) or siRNA-resistant NXF1-Escape mutants (ESC1 or ESC2). Viral RNA (unspliced and spliced), GAPDH, and rRNA in each sample are shown. Western blot analysis was also performed to verify siRNA-mediated NXF1 knockdown as well as the resistance of the NXF1-Escape mutant to siRNA treatment. β-Actin and GAPDH were also detected by specific antibodies as loading controls. (B) Deep sequencing analysis of viral (*pol* and *env*) and cellular (NXF1, β-actin, and GAPDH) mRNAs in persistently MLV-infected TE671 cells. Fold changes after treatment with siRNA are summarized (∗, $P < 0.05$). Error bars indicate standard deviations ($n = 3$).

The MLV leader sequence modulates the splicing efficiency of viral transcripts, and NXF1 mediates the cytoplasmic accumulation of spliced and unspliced MLV transcripts. We also assessed the influence of NXF1 depletion on transient MLV gene expression in 293T cells transiently transfected with an infectious molecular clone of AM-MLV, pAMS. Disruption of NXF1 expression reduced the levels of MLV Gag and Env expression (Fig. 8A) as well as the cytoplasmic levels of MLV transcripts (Fig. 8B). Unlike TE671 cells, disruption of NXF1 expression in 293T cells resulted in extensive degradation of the MLV transcripts in the nuclei (Fig. 8B), whereas full-exome sequencing analysis demonstrated little effect of NXF1 depletion on the cellular RNA reads in 293T cells (data not shown).

Previous studies have demonstrated the importance of the 5′ UTR for the alternative splicing of MLV transcripts; the PBS activates splicing, while flanking sequences downstream of the PBS (3′ PBS) are inhibitory (21). We generated the MLV splicing mutants pAMSΔPBS and pAMSΔ3′PBS based on the pAMS plasmid (Fig. 8C). Transfection of pAMSΔPBS and pAMSΔ3′PBS showed reduced and accelerated splicing patterns in the nucleus, respectively (Fig. 8C). When knockdown effects of NXF1 were examined by using these constructs, depletion of NXF1 arrested the export of spliced and unspliced viral transcripts, resulting in an accumulation of degraded viral transcripts in the nucleus (Fig. 8D). The nuclear degradation of viral transcripts was unique to the NXF1-depleted cells; no notable degradation of viral transcripts was observed with control siRNA or siRNA against a recently identified adaptor protein, germinal center-associated nuclear protein (GANP) (51) (Fig. 8D, right). These observations confirmed that both spliced and unspliced MLV transcripts were exported through the NXF1 pathway. Furthermore, our data suggest that NXF1 also stabilizes viral RNA in the nucleus.

DISCUSSION

In this study, we examined the mechanisms underlying the nuclear export of gammaretrovirus RNA transcripts. Our results demonstrate that gammaretroviruses have a conserved *cis*-acting element, the CAE, in the *pol* gene, which enhances the cytoplasmic accumulation of viral transcripts and expression of viral proteins in an NXF1-dependent manner. NXF1 also interacted with intron-containing, unspliced transcripts of gammaretroviruses. Disruption of NXF1 expression impaired cytoplasmic accumulations of both spliced and unspliced transcripts of XMRV and MLV, resulting in their nuclear retention or degradation. Based on these observations, we concluded that gammaretroviruses use NXF1 for the cytoplasmic accumulation of spliced and unspliced viral transcripts.

The *env* leader sequences of Moloney MLV (52) and murine intracisternal A-type particle (IAP) MIA14 (53) have been shown to enhance the cytoplasmic accumulation of viral transcripts. The insertion of the IAP element can replace the function of the CTE or RRE in a Rev-independent HIV Gag expression system (53). Here, we demonstrated that the CAE sequence enhanced the cytoplasmic accumulation of XMRV *env* transcripts (Fig. 2D) without affecting the splicing patterns (Fig. 2A), the half-life of viral transcripts (Fig. 2B), or the translation efficiency of the transcripts (Fig. 2C). The introduction of the CAE sequence rescued Rev-independent HIV-1 Gag expression (Fig. 3). Further mapping

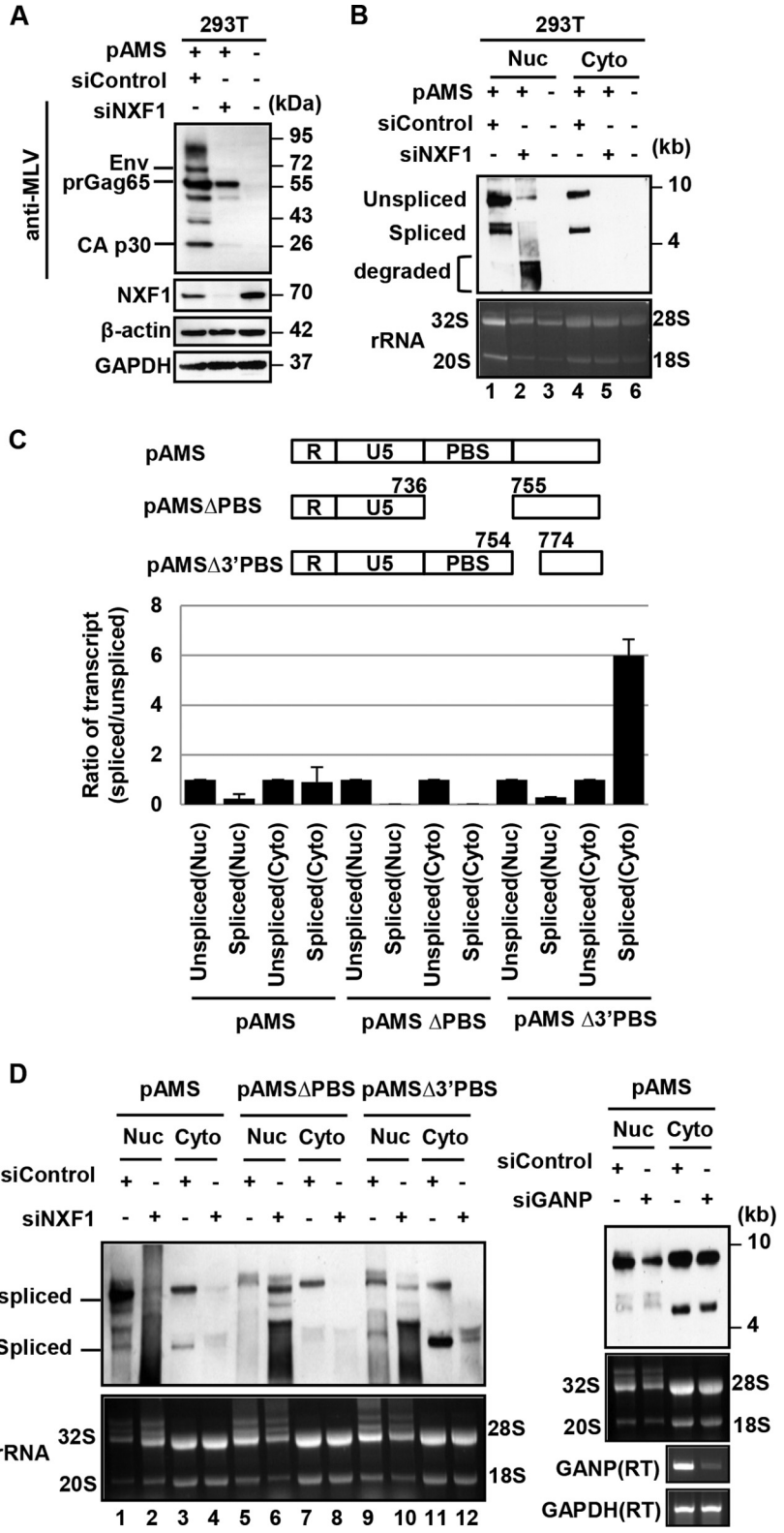

FIG 8 The MLV leader sequence modulates the splicing efficiency of viral transcripts, and NXF1 mediates the cytoplasmic accumulation of spliced and unspliced MLV transcripts. (A) Western blot analysis was performed to determine the influence of NXF1 disruption on transient MLV protein expression in 293T cells. Cells were transfected with the indicated siRNAs, followed by transfection with 0.4 μg of plasmid. Cells were harvested 48 h after siRNA transfection for protein expression analysis using the indicated antibodies. (B) Northern blotting of MLV transcripts in 293T cells. Cells were transfected with pAMS and treated with the indicated siRNA. Viral transcripts and rRNAs from nuclear and cytoplasmic fractions are indicated as loading controls. Note the extensive degradation of viral transcripts in the nucleus upon NXF1 depletion. (C) Schematic representation of the 5′ LTR region of pAMS. In the PBS deletion mutant pAMSΔPBS, the PBS

identified the 9-nt core CAE sequence (GGAAAGGAC) essential for CAE function (Fig. 4F). Our observations indicate that the region downstream of the *env* splice acceptor site in gammaretroviruses plays an important role in the nucleocytoplasmic transport of viral transcripts.

NXF1 is recruited to fully spliced mRNAs through interactions with various adaptor proteins, such as UAP56, Aly/REF, and a transcription/export (TREX) complex, to facilitate the export of different mRNA classes (51, 54). Although NXF1 binds RNA through its N-terminal RNA-binding domain (RBD), the NXF1 RBD has no clear sequence specificity and shows promiscuous interactions with a variety of RNA substrates (55, 56). A recent study suggests that NXF1 uses an intramolecular interaction to block its RNA-binding activity, which is released by a conformational change upon contact with Aly/REF and a TREX subunit (57). In contrast, the modes of NXF1 interaction with viral RNAs are different. For instance, influenza virus RNAs directly bind NXF1 (58). Similarly, the CTEs of betaretroviruses directly bind NXF1 to facilitate the export of intron-containing viral transcripts (59, 60). The NXF1-mediated recognition of the CTE RNA is highly sequence specific. The RBD and leucine-rich repeat motifs of NXF1 bind to one symmetrical half of the CTE RNA with L-shaped conformations to facilitate export (61), while the introduction of point mutations into the CTE sequence abolishes the interaction (61, 62). Here, we demonstrated that a short-term, modest NXF1 disruption significantly reduced cytoplasmic, but not nuclear, levels of MLV transcripts (Fig. 6E and 7B). Notably, the overexpression of siRNA-resistant NXF1 significantly enhanced cytoplasmic accumulations of MLV transcripts (Fig. 7B) without significantly affecting other cellular transcript reads (not shown). These observations suggest that the cytoplasmic accumulation of MLV transcripts requires higher levels of NXF1 than cellular transcripts. The higher NXF1 dependency may be due to the differences in the use of NXF1 adaptor proteins, such as Aly/REF, between gammaretroviral and cellular transcripts. Because the comparison of the CAE sequence with the CTEs showed no conserved sequence, it currently remains to be determined if the CAEs play precisely the same role as CTEs. Our preliminary studies found no evidence of a direct interaction between the CAE sequence and NXF1. However, this experiment is not straightforward, as NXF1 likely functions as a heterodimer with NXT1. We are currently examining the involvement of adaptor proteins and NXT1 in the CAE-NXF1 interaction.

Intron-containing cellular mRNAs are subject to restricted nuclear export in higher eukaryotes (63). Previous studies have demonstrated that modulation of the viral 5′ leader sequence affects the cytoplasmic accumulation of spliced and unspliced MLV transcripts. For instance, deletion of the first 28 nt of the R region is critical for the cytoplasmic level of unspliced full-length viral transcripts (20, 64), while deletions in the PBS sequence also modulate the balance between unspliced and spliced MLV transcripts (21). We generated MLV mutants with the same mutations as those reported previously by Kraunus et al. (21) and confirmed that the deletions of the PBS or the region between the PBS and SD site reduced or increased the levels of spliced transcripts in the nucleus. Nevertheless, disruption of NXF1 blocked the cytoplasmic accumulations of spliced and unspliced gammaretroviral transcripts from these mutants. These observations indicate that MLV uses the sequences upstream of the 5′ major SD site to control the cytoplasmic accumulation of the intron-containing viral transcripts, primarily through modulation of the splicing efficiency but not through utilization of different nuclear export pathways. Given that the upstream splice donor and downstream splice acceptor regions are targeted by cellular splicing machinery, it may not be surprising that both the viral 5′ leader sequence, located immediately upstream of the SD site, and the CAE sequence, located downstream of the SA site, play critical roles in regulating the splicing and export of MLV transcripts.

NXF1 is implicated as a factor licensing the nuclear export of spliced mRNAs (65) as well as unspliced mRNAs (66). In 293T cells, NXF1 depletion not only blocked the cytoplasmic accumulation of gammaretroviral transcripts but also induced notable intranuclear degradation of viral transcripts (Fig. 8B), suggesting that NXF1 binding protects MLV transcripts from degradation in the nucleus. Since recruitment of RNA-binding proteins protects mRNA from degradation by the nuclear RNA surveillance machineries, such as the nuclear exosome (67), NXF1 may play a role in determining the fates of gammaretroviral transcripts for "protection and export" or "degradation," thereby linking RNA export and surveillance. In this context, it is also notable that NXF1 depletion increased the cytoplasmic accumulation of aberrantly spliced transcripts (Fig. 8D). Since the same-sized bands were observed in cells transfected with a wild-type MLV clone without NXF1, these bands are likely splice intermediates or minor alternatively spliced transcripts, which can be produced even in normal 293T cells during wild-type MLV production. Nevertheless, NXF1 depletion potently inhibited nuclear export of properly spliced transcripts yet allowed the export of aberrantly spliced transcripts, implying NXF1's role as a factor controlling the proper processing and export of MLV transcripts. It is plausible that disruption of NXF1 may lead to failed RNA surveillance, which accelerates nuclear export of aberrantly processed transcripts through an NXF1-independent pathway.

A potential issue with the use of RNA interference (RNAi)-mediated NXF1 disruption is the indirect effects induced by sustained NXF1 disruption. Transfection of an NXF1 siRNA can reduce (i) NXF1 transcript levels, (ii) NXF1 protein levels, (iii) nuclear export of NXF1-dependent viral/cellular mRNAs, and, ultimately, (iv) protein levels of NXF1-dependent viral/cellular factors, leading to nonspecific indirect effects. To minimize this, we determined the influence of NXF1 disruption 48 h after siRNA transfection. At 48 h, we observed little effect on cellular protein

region (nt positions 737 to 754, based on GenBank accession number AF010170) was deleted. In the pAMSΔ3′PBS construct, the sequence immediately downstream of the PBS (nt positions 755 to 773) was deleted. After Northern blot analysis in 293T cells, the intensity of the unspliced and spliced bands was quantified by using ImageJ software, and the ratios of spliced/unspliced transcripts were determined. The level of unspliced RNA was set to 1. Ratios of unspliced to spliced transcripts were 1:0.24 for pAMS (nuclear), 1:0.9 for pAMS (cytoplasmic), 1:0.0012 for pAMSΔPBS (nuclear), 1:0.0167 for pAMSΔPBS (cytoplasmic), 1:0.3 for pAMSΔ3′PBS (nuclear), and 1:6 for pAMSΔ3′PBS (cytoplasmic). Error bars represent standard errors of two independent experiments. (D) Northern blot analysis of MLV transcripts in 293T cells transfected with pAMS, pAMSΔPBS, or pAMSΔ3′PBS, with or without treatment with NXF1- or GANP-targeting siRNAs. Agarose gel images of ethidium bromide-stained rRNAs, including 45S, 32S, and 20S in the nucleus and 28S and 18S in the cytoplasm, are also shown. Silencing of GANP was verified by RT-PCR with GAPDH as the internal control.

levels, including beta-actin (Fig. 5H), as well as accumulated viral Gag polyproteins (Fig. 5H). Similar "short-term NXF1 disruption" protocols have been used to study the contribution of NXF1 to the nuclear export of cellular and viral transcripts (57, 58, 68, 69). Our full-exome sequencing study also demonstrated that transfection of the NXF1 siRNA for 48 h reduced cytoplasmic NXF1 transcript levels by 75% (Fig. 7B). This modest NXF1 disruption did not significantly affect the cytoplasmic accumulations of the majority of cellular transcripts: only 121 genes out of 11,729 cellular genes showed >4-fold downregulation in the cytoplasm upon transfection of NXF1 siRNA. These data verified that our NXF1 disruption experiments had minimal indirect effects.

Transfection of *in vitro*-translated mRNAs has been widely used to assess the stability or translational capacity of mutated mRNAs in the cytoplasm. However, RNA export is often coupled to translation (70), and therefore, it remains possible that the CAE sequence also influences translation efficiency.

In summary, we demonstrate that MLV uses NXF1 for the nuclear export of both spliced and unspliced viral RNA transcripts. Unlike HIV-1, MLV regulates the cytoplasmic accumulation of intron-containing MLV transcripts primarily at the splicing step through leader sequence-mediated splicing modulation.

ACKNOWLEDGMENTS

This work was supported by the National Institutes of Health (AI093186) and the Mayo Foundation (Y.I.).

The infectious molecular clone of XMRV, pVP62/pcDNA3.1(−), was a kind gift from Robert H. Silverman (Cleveland Clinic, OH). pHRSINCSGW_PGRPuro was kindly provided by Paul Lehner (Cambridge Institute for Medical Research, United Kingdom). We thank Greg J. Towers (University College London, United Kingdom) and Blair L. Strang (St. George's Medical School, University of London) for critical reading of the manuscript.

T.S. and Y.I. conceived of and designed the experiments. T.S., J.A.M., and J.M.T. performed the experiments. T.S. and Y.I. analyzed the data. T.S. and Y.I. wrote the paper. T.S., J.M.T., and Y.I. edited the manuscript.

We declare that we have no conflict of interest.

REFERENCES

1. **Ner-Gaon H, Halachmi R, Savaldi-Goldstein S, Rubin E, Ophir R, Fluhr R.** 2004. Intron retention is a major phenomenon in alternative splicing in Arabidopsis. Plant J. **39:**877–885. http://dx.doi.org/10.1111/j.1365-313X.2004.02172.x.
2. **Indik S, Gunzburg WH, Salmons B, Rouault F.** 2005. A novel, mouse mammary tumor virus encoded protein with Rev-like properties. Virology **337:**1–6. http://dx.doi.org/10.1016/j.virol.2005.03.040.
3. **Sakuma T, Barry MA, Ikeda Y.** 2012. Lentiviral vectors: basic to translational. Biochem. J. **443:**603–618. http://dx.doi.org/10.1042/BJ20120146.
4. **Sandri-Goldin RM.** 2004. Viral regulation of mRNA export. J. Virol. **78:**4389–4396. http://dx.doi.org/10.1128/JVI.78.9.4389-4396.2004.
5. **Cullen BR.** 2005. Human immunodeficiency virus: nuclear RNA export unwound. Nature **433:**26–27. http://dx.doi.org/10.1038/433026a.
6. **Zapp ML, Green MR.** 1989. Sequence-specific RNA binding by the HIV-1 Rev protein. Nature **342:**714–716. http://dx.doi.org/10.1038/342714a0.
7. **Daly TJ, Cook KS, Gray GS, Maione TE, Rusche JR.** 1989. Specific binding of HIV-1 recombinant Rev protein to the Rev-responsive element in vitro. Nature **342:**816–819. http://dx.doi.org/10.1038/342816a0.
8. **Popa I, Harris ME, Donello JE, Hope TJ.** 2002. CRM1-dependent function of a cis-acting RNA export element. Mol. Cell. Biol. **22:**2057–2067. http://dx.doi.org/10.1128/MCB.22.7.2057-2067.2002.
9. **Ahmed YF, Hanly SM, Malim MH, Cullen BR, Greene WC.** 1990. Structure-function analyses of the HTLV-I Rex and HIV-1 Rev RNA response elements: insights into the mechanism of Rex and Rev action. Genes Dev. **4:**1014–1022.
10. **Hanly SM, Rimsky LT, Malim MH, Kim JH, Hauber J, Duc Dodon M, Le SY, Maizel JV, Cullen BR, Greene WC.** 1989. Comparative analysis of the HTLV-I Rex and HIV-1 Rev trans-regulatory proteins and their RNA response elements. Genes Dev. **3:**1534–1544. http://dx.doi.org/10.1101/gad.3.10.1534.
11. **Mertz JA, Simper MS, Lozano MM, Payne SM, Dudley JP.** 2005. Mouse mammary tumor virus encodes a self-regulatory RNA export protein and is a complex retrovirus. J. Virol. **79:**14737–14747. http://dx.doi.org/10.1128/JVI.79.23.14737-14747.2005.
12. **Nitta T, Hofacre A, Hull S, Fan H.** 2009. Identification and mutational analysis of a Rej response element in Jaagsiekte sheep retrovirus RNA. J. Virol. **83:**12499–12511. http://dx.doi.org/10.1128/JVI.01754-08.
13. **Bodem J, Schied T, Gabriel R, Rammling M, Rethwilm A.** 2011. Foamy virus nuclear RNA export is distinct from that of other retroviruses. J. Virol. **85:**2333–2341. http://dx.doi.org/10.1128/JVI.01518-10.
14. **Bray M, Prasad S, Dubay JW, Hunter E, Jeang KT, Rekosh D, Hammarskjold ML.** 1994. A small element from the Mason-Pfizer monkey virus genome makes human immunodeficiency virus type 1 expression and replication Rev-independent. Proc. Natl. Acad. Sci. U. S. A. **91:**1256–1260. http://dx.doi.org/10.1073/pnas.91.4.1256.
15. **Swanson CM, Puffer BA, Ahmad KM, Doms RW, Malim MH.** 2004. Retroviral mRNA nuclear export elements regulate protein function and virion assembly. EMBO J. **23:**2632–2640. http://dx.doi.org/10.1038/sj.emboj.7600270.
16. **Li Y, Bor YC, Misawa Y, Xue Y, Rekosh D, Hammarskjold ML.** 2006. An intron with a constitutive transport element is retained in a Tap messenger RNA. Nature **443:**234–237. http://dx.doi.org/10.1038/nature05107.
17. **Yang J, Cullen BR.** 1999. Structural and functional analysis of the avian leukemia virus constitutive transport element. RNA **5:**1645–1655. http://dx.doi.org/10.1017/S1355838299991616.
18. **Paca RE, Ogert RA, Hibbert CS, Izaurralde E, Beemon KL.** 2000. Rous sarcoma virus DR posttranscriptional elements use a novel RNA export pathway. J. Virol. **74:**9507–9514. http://dx.doi.org/10.1128/JVI.74.20.9507-9514.2000.
19. **LeBlanc JJ, Uddowla S, Abraham B, Clatterbuck S, Beemon KL.** 2007. Tap and Dbp5, but not Gag, are involved in DR-mediated nuclear export of unspliced Rous sarcoma virus RNA. Virology **363:**376–386. http://dx.doi.org/10.1016/j.virol.2007.01.026.
20. **Trubetskoy AM, Okenquist SA, Lenz J.** 1999. R region sequences in the long terminal repeat of a murine retrovirus specifically increase expression of unspliced RNAs. J. Virol. **73:**3477–3483.
21. **Kraunus J, Zychlinski D, Heise T, Galla M, Bohne J, Baum C.** 2006. Murine leukemia virus regulates alternative splicing through sequences upstream of the 5′ splice site. J. Biol. Chem. **281:**37381–37390. http://dx.doi.org/10.1074/jbc.M601537200.
22. **Sakuma T, Ravin SS, Tonne JM, Thatava T, Ohmine S, Takeuchi Y, Malech HL, Ikeda Y.** 2010. Characterization of retroviral and lentiviral vectors pseudotyped with XMRV envelope glycoprotein. Hum. Gene Ther. **21:**1665–1673. http://dx.doi.org/10.1089/hum.2010.063.
23. **Miller AD, Law MF, Verma IM.** 1985. Generation of helper-free amphotropic retroviruses that transduce a dominant-acting, methotrexate-resistant dihydrofolate reductase gene. Mol. Cell. Biol. **5:**431–437.
24. **Tsai MC, Manor O, Wan Y, Mosammaparast N, Wang JK, Lan F, Shi Y, Segal E, Chang HY.** 2010. Long noncoding RNA as modular scaffold of histone modification complexes. Science **329:**689–693. http://dx.doi.org/10.1126/science.1192002.
25. **Sakuma R, Sakuma T, Ohmine S, Silverman RH, Ikeda Y.** 2010. Xenotropic murine leukemia virus-related virus is susceptible to AZT. Virology **397:**1–6. http://dx.doi.org/10.1016/j.virol.2009.11.013.
26. **Sakuma T, Hue S, Squillace KA, Tonne JM, Blackburn PR, Ohmine S, Thatava T, Towers GJ, Ikeda Y.** 2011. No evidence of XMRV in prostate cancer cohorts in the Midwestern United States. Retrovirology **8:**23. http://dx.doi.org/10.1186/1742-4690-8-23.
27. **Wang L, Wang S, Li W.** 2012. RSeQC: quality control of RNA-seq experiments. Bioinformatics **28:**2184–2185. http://dx.doi.org/10.1093/bioinformatics/bts356.
28. **Trapnell C, Pachter L, Salzberg SL.** 2009. TopHat: discovering splice junctions with RNA-Seq. Bioinformatics **25:**1105–1111. http://dx.doi.org/10.1093/bioinformatics/btp120.
29. **Langmead B, Trapnell C, Pop M, Salzberg SL.** 2009. Ultrafast and memory-

efficient alignment of short DNA sequences to the human genome. Genome Biol. **10:**R25. http://dx.doi.org/10.1186/gb-2009-10-3-r25.
30. **Li H, Durbin R.** 2009. Fast and accurate short read alignment with Burrows-Wheeler transform. Bioinformatics **25:**1754–1760. http://dx.doi.org/10.1093/bioinformatics/btp324.
31. **McKenna A, Hanna M, Banks E, Sivachenko A, Cibulskis K, Kernytsky A, Garimella K, Altshuler D, Gabriel S, Daly M, DePristo MA.** 2010. The Genome Analysis Toolkit: a MapReduce framework for analyzing next-generation DNA sequencing data. Genome Res. **20:**1297–1303. http://dx.doi.org/10.1101/gr.107524.110.
32. **Robinson MD, McCarthy DJ, Smyth GK.** 2010. edgeR: a Bioconductor package for differential expression analysis of digital gene expression data. Bioinformatics **26:**139–140. http://dx.doi.org/10.1093/bioinformatics/btp616.
33. **Berlioz C, Darlix JL.** 1995. An internal ribosomal entry mechanism promotes translation of murine leukemia virus gag polyprotein precursors. J. Virol. **69:**2214–2222.
34. **Carroll R, Derse D.** 1993. Translation of equine infectious anemia virus bicistronic tat-rev mRNA requires leaky ribosome scanning of the tat CTG initiation codon. J. Virol. **67:**1433–1440.
35. **Ernst RK, Bray M, Rekosh D, Hammarskjold ML.** 1997. Secondary structure and mutational analysis of the Mason-Pfizer monkey virus RNA constitutive transport element. RNA **3:**210–222.
36. **Tabernero C, Zolotukhin AS, Valentin A, Pavlakis GN, Felber BK.** 1996. The posttranscriptional control element of the simian retrovirus type 1 forms an extensive RNA secondary structure necessary for its function. J. Virol. **70:**5998–6011.
37. **Singh R, Green MR.** 1993. Sequence-specific binding of transfer RNA by glyceraldehyde-3-phosphate dehydrogenase. Science **259:**365–368. http://dx.doi.org/10.1126/science.8420004.
38. **Mingot JM, Kostka S, Kraft R, Hartmann E, Gorlich D.** 2001. Importin 13: a novel mediator of nuclear import and export. EMBO J. **20:**3685–3694. http://dx.doi.org/10.1093/emboj/20.14.3685.
39. **Kutay U, Bischoff FR, Kostka S, Kraft R, Gorlich D.** 1997. Export of importin alpha from the nucleus is mediated by a specific nuclear transport factor. Cell **90:**1061–1071. http://dx.doi.org/10.1016/S0092-8674(00)80372-4.
40. **Kurisaki A, Kurisaki K, Kowanetz M, Sugino H, Yoneda Y, Heldin CH, Moustakas A.** 2006. The mechanism of nuclear export of Smad3 involves exportin 4 and Ran. Mol. Cell. Biol. **26:**1318–1332. http://dx.doi.org/10.1128/MCB.26.4.1318-1332.2006.
41. **Lipowsky G, Bischoff FR, Schwarzmaier P, Kraft R, Kostka S, Hartmann E, Kutay U, Gorlich D.** 2000. Exportin 4: a mediator of a novel nuclear export pathway in higher eukaryotes. EMBO J. **19:**4362–4371. http://dx.doi.org/10.1093/emboj/19.16.4362.
42. **Brownawell AM, Macara IG.** 2002. Exportin-5, a novel karyopherin, mediates nuclear export of double-stranded RNA binding proteins. J. Cell Biol. **156:**53–64. http://dx.doi.org/10.1083/jcb.200110082.
43. **Bohnsack MT, Regener K, Schwappach B, Saffrich R, Paraskeva E, Hartmann E, Gorlich D.** 2002. Exp5 exports eEF1A via tRNA from nuclei and synergizes with other transport pathways to confine translation to the cytoplasm. EMBO J. **21:**6205–6215. http://dx.doi.org/10.1093/emboj/cdf613.
44. **Calado A, Treichel N, Muller EC, Otto A, Kutay U.** 2002. Exportin-5-mediated nuclear export of eukaryotic elongation factor 1A and tRNA. EMBO J. **21:**6216–6224. http://dx.doi.org/10.1093/emboj/cdf620.
45. **Gwizdek C, Ossareh-Nazari B, Brownawell AM, Doglio A, Bertrand E, Macara IG, Dargemont C.** 2003. Exportin-5 mediates nuclear export of minihelix-containing RNAs. J. Biol. Chem. **278:**5505–5508. http://dx.doi.org/10.1074/jbc.C200668200.
46. **Stade K, Ford CS, Guthrie C, Weis K.** 1997. Exportin 1 (Crm1p) is an essential nuclear export factor. Cell **90:**1041–1050. http://dx.doi.org/10.1016/S0092-8674(00)80370-0.
47. **Fornerod M, Ohno M, Yoshida M, Mattaj IW.** 1997. CRM1 is an export receptor for leucine-rich nuclear export signals. Cell **90:**1051–1060. http://dx.doi.org/10.1016/S0092-8674(00)80371-2.
48. **Stuven T, Hartmann E, Gorlich D.** 2003. Exportin 6: a novel nuclear export receptor that is specific for profilin.actin complexes. EMBO J. **22:**5928–5940. http://dx.doi.org/10.1093/emboj/cdg565.
49. **Mingot JM, Bohnsack MT, Jakle U, Gorlich D.** 2004. Exportin 7 defines a novel general nuclear export pathway. EMBO J. **23:**3227–3236. http://dx.doi.org/10.1038/sj.emboj.7600338.
50. **Paprotka T, Delviks-Frankenberry KA, Cingoz O, Martinez A, Kung HJ, Tepper CG, Hu WS, Fivash MJ, Jr, Coffin JM, Pathak VK.** 2011. Recombinant origin of the retrovirus XMRV. Science **333:**97–101. http://dx.doi.org/10.1126/science.1205292.
51. **Wickramasinghe VO, McMurtrie PI, Mills AD, Takei Y, Penrhyn-Lowe S, Amagase Y, Main S, Marr J, Stewart M, Laskey RA.** 2010. mRNA export from mammalian cell nuclei is dependent on GANP. Curr. Biol. **20:**25–31. http://dx.doi.org/10.1016/j.cub.2009.10.078.
52. **Oshima M, Odawara T, Matano T, Sakahira H, Kuchino Y, Iwamoto A, Yoshikura H.** 1996. Possible role of splice acceptor site in expression of unspliced gag-containing message of Moloney murine leukemia virus. J. Virol. **70:**2286–2295.
53. **Wodrich H, Bohne J, Gumz E, Welker R, Krausslich HG.** 2001. A new RNA element located in the coding region of a murine endogenous retrovirus can functionally replace the Rev/Rev-responsive element system in human immunodeficiency virus type 1 Gag expression. J. Virol. **75:**10670–10682. http://dx.doi.org/10.1128/JVI.75.22.10670-10682.2001.
54. **Rodrigues JP, Rode M, Gatfield D, Blencowe BJ, Carmo-Fonseca M, Izaurralde E.** 2001. REF proteins mediate the export of spliced and unspliced mRNAs from the nucleus. Proc. Natl. Acad. Sci. U. S. A. **98:**1030–1035. http://dx.doi.org/10.1073/pnas.98.3.1030.
55. **Zolotukhin AS, Tan W, Bear J, Smulevitch S, Felber BK.** 2002. U2AF participates in the binding of TAP (NXF1) to mRNA. J. Biol. Chem. **277:**3935–3942. http://dx.doi.org/10.1074/jbc.M107598200.
56. **Hautbergue GM, Hung ML, Walsh MJ, Snijders AP, Chang CT, Jones R, Ponting CP, Dickman MJ, Wilson SA.** 2009. UIF, a new mRNA export adaptor that works together with REF/ALY, requires FACT for recruitment to mRNA. Curr. Biol. **19:**1918–1924. http://dx.doi.org/10.1016/j.cub.2009.09.041.
57. **Viphakone N, Hautbergue GM, Walsh M, Chang CT, Holland A, Folco EG, Reed R, Wilson SA.** 2012. TREX exposes the RNA-binding domain of Nxf1 to enable mRNA export. Nat. Commun. **3:**1006. http://dx.doi.org/10.1038/ncomms2005.
58. **Morita M, Kuba K, Ichikawa A, Nakayama M, Katahira J, Iwamoto R, Watanebe T, Sakabe S, Daidoji T, Nakamura S, Kadowaki A, Ohto T, Nakanishi H, Taguchi R, Nakaya T, Murakami M, Yoneda Y, Arai H, Kawaoka Y, Penninger JM, Arita M, Imai Y.** 2013. The lipid mediator protectin D1 inhibits influenza virus replication and improves severe influenza. Cell **153:**112–125. http://dx.doi.org/10.1016/j.cell.2013.02.027.
59. **Gruter P, Tabernero C, von Kobbe C, Schmitt C, Saavedra C, Bachi A, Wilm M, Felber BK, Izaurralde E.** 1998. TAP, the human homolog of Mex67p, mediates CTE-dependent RNA export from the nucleus. Mol. Cell **1:**649–659. http://dx.doi.org/10.1016/S1097-2765(00)80065-9.
60. **Braun IC, Rohrbach E, Schmitt C, Izaurralde E.** 1999. TAP binds to the constitutive transport element (CTE) through a novel RNA-binding motif that is sufficient to promote CTE-dependent RNA export from the nucleus. EMBO J. **18:**1953–1965. http://dx.doi.org/10.1093/emboj/18.7.1953.
61. **Teplova M, Wohlbold L, Khin NW, Izaurralde E, Patel DJ.** 2011. Structure-function studies of nucleocytoplasmic transport of retroviral genomic RNA by mRNA export factor TAP. Nat. Struct. Mol. Biol. **18:**990–998. http://dx.doi.org/10.1038/nsmb.2094.
62. **Kang Y, Cullen BR.** 1999. The human Tap protein is a nuclear mRNA export factor that contains novel RNA-binding and nucleocytoplasmic transport sequences. Genes Dev. **13:**1126–1139. http://dx.doi.org/10.1101/gad.13.9.1126.
63. **Luo MJ, Reed R.** 1999. Splicing is required for rapid and efficient mRNA export in metazoans. Proc. Natl. Acad. Sci. U. S. A. **96:**14937–14942. http://dx.doi.org/10.1073/pnas.96.26.14937.
64. **Cupelli L, Okenquist SA, Trubetskoy A, Lenz J.** 1998. The secondary structure of the R region of a murine leukemia virus is important for stimulation of long terminal repeat-driven gene expression. J. Virol. **72:**7807–7814.
65. **Cullen BR.** 2000. Connections between the processing and nuclear export of mRNA: evidence for an export license? Proc. Natl. Acad. Sci. U. S. A. **97:**4–6. http://dx.doi.org/10.1073/pnas.97.1.4.
66. **Lei H, Dias AP, Reed R.** 2011. Export and stability of naturally intronless mRNAs require specific coding region sequences and the TREX mRNA export complex. Proc. Natl. Acad. Sci. U. S. A. **108:**17985–17990. http://dx.doi.org/10.1073/pnas.1113076108.
67. **Anko ML, Neugebauer KM.** 2012. RNA-protein interactions in vivo: global gets specific. Trends Biochem. Sci. **37:**255–262. http://dx.doi.org/10.1016/j.tibs.2012.02.005.
68. **Johnson LA, Sandri-Goldin RM.** 2009. Efficient nuclear export of herpes simplex virus 1 transcripts requires both RNA binding by ICP27 and

ICP27 interaction with TAP/NXF1. J. Virol. **83:**1184–1192. http://dx.doi.org/10.1128/JVI.02010-08.
69. **Kim M, Bellini M, Ceman S.** 2009. Fragile X mental retardation protein FMRP binds mRNAs in the nucleus. Mol. Cell. Biol. **29:**214–228. http://dx.doi.org/10.1128/MCB.01377-08.
70. **Jin L, Guzik BW, Bor YC, Rekosh D, Hammarskjold ML.** 2003. Tap and NXT promote translation of unspliced mRNA. Genes Dev. **17:**3075–3086. http://dx.doi.org/10.1101/gad.1155703.
71. **Sakuma T, Tonne JM, Squillace KA, Ohmine S, Thatava T, Peng KW, Barry MA, Ikeda Y.** 2011. Early events in retrovirus XMRV infection of the wild-derived mouse Mus pahari. J. Virol. **85:**1205–1213. http://dx.doi.org/10.1128/JVI.00886-10.